ISSN NO. 2320-5407

Journal homepage: http://www.journalijar.com

INTERNATIONAL JOURNAL OF ADVANCED RESEARCH

RESEARCH ARTICLE

CO oxidation over various nanostructured metal oxides

M.H.Khedr[1], M.I.Nasr[2], K.S.Abdel Halim[2],A.A.Farghali[1], N.K.Soliman[3,*]

1 Chemistry Department, Faculty of Science, Beni-Suef University, Beni-Suef, Egypt

2 Central Metallurgical Research and Development Institute (CMRDI), Minerals Technology, 87 Helwan, Cairo, Egypt

3 Basic Science Department, Faculty of Oral and Dental Medicine, Nahda university (NUB),Beni-suef ,Egypt

Manuscript Info

Manuscript History:

Received: 12 May 2014
Final Accepted: 12 June 2014
Published Online: July 2014

Key words:
CO oxidation; Nanostructure; metal Oxides; Chemical synthesis; Microstructure

Corresponding Author

N.K.Soliman

Abstract

Nanosized CuO-CeO_2, CuO-Fe_2O_3, CuO-CeO_2-Al_2O_3 and CuO-Fe_2O_3-CeO_2-Al_2O_3 were successfully prepared by co-precipitation and wet impregnations techniques and tested for the catalytic oxidation of CO to CO_2. The influence of different factors as catalyst chemical structure, catalytic temperature and weight of catalyst on the rate of catalytic reaction was investigated using advanced quadruple mass gas analyzer system. It can be reported that the rate of conversion of CO to CO_2 is affected by the catalyst chemical structure where the maximum CO conversion % occurs over ceria containing catalysts all the catalytic temperatures and increase with increasing catalytic temperature from 300-400^oC, it reach about 100% at 400^oC, and over these temperature range, CO conversion % decreases as a result of sintering effect. CO inlet concentration and catalyst mass also affect on the rate of conversion of CO to CO_2 where CO conversion % increase with increasing catalyst mass and decreasing CO inlet concentration. The catalytic oxidation of CO to CO_2 is probably proceed by adsorption mechanism where the reactants are adsorbed on the surface of the catalyst with breaking O–O bonds, then CO pick up the dissociated O atom forming CO_2.

Introduction

Carbon monoxide is one of the main pollutants released from internal combustion engines and is the source of many environmental and health problems (GLOBAL; Mathers et al., 2009). For example, Carbon monoxide gas is strongly binds to the iron atom in blood hemoglobin and so the hemoglobin becomes incapable of releasing oxygen. A sufficient exposure to carbon monoxide can reduce the amount of oxygen taken up by the brain to the point that the victim becomes unconscious, and can suffer brain damage or even death from anoxia (Organization, 1999). The catalytic oxidation of CO to CO_2 at ambient temperatures is of importance in the control of environmental pollution and it has extensive applications in many fields such as automotive exhaust emission control, mine rescue devices, and traceable CO removal in enclosed atmospheres.

Previously the oxidation of CO to CO_2 is catalyzed over noble metals as gold and platinum. The cost of these noble metals does not make it economically feasible to be used. This had lead to searching for other catalysts which are cheaper and more abundant. In addition to being economically feasible to be used nanosized materials are characterized by unique, essential and important applications especially in the field of catalysis and recently metal oxides nanoparticles such as Cupper oxides , and iron oxide alone or in combination with supported materials like CeO_2 and/or Al_2O_3 are found to be promising and effective catalysts for CO oxidation (Abdel Halim et al., 2007; Avgouropoulos et al., 2001; Dudfield et al., 2001; Gulyaev et al., 2014; Halim et al., 2008; Kang et al., 2013; Khedr et al., 2006; Martynova et al., 2013; Pérez et al., 2013; Rashad et al., 2006; Reddy et al., 2004b; Teng et al., 1999; Xia et al., 1999).

The catalyst used in oxidation of CO to CO_2 must have high CO oxidation activity, high selectivity, and good resistance towards deactivation by H_2O and CO_2 (Choudhary and Goodman, 2002; Trimm and Ã–nsan, 2001). The catalytic activity of synthesized metal oxide catalysts has a great dependence on the preparation methods, including co-precipitation (Kim and Cha, 2003), combustion method (Shan et al., 2004), sol–gel route(Avgouropoulos et al., 2002) and others.

Catalyst crystallite size and catalytic temperature have a great influence on CO oxidation process ,K.S.Abdel-Halim et al (Abdel Halim et al., 2007) investigated the Factors affecting CO oxidation over nano-sized Fe_2O_3 and they found that CO conversion % decreased with the increasing of crystallite size of the prepared samples and that the catalytic temperature plays a significant role in the oxidation of CO to CO_2. The reaction was found to be first order with respect to CO and probably proceed by adsorption mechanism where the reactants are adsorbed on the surface of the catalyst with breaking O-O bonds, then CO pick up the dissociated O atom forming CO_2. It was found also that the using of ethanol as dehydrating agent in co-precipitation technique led to prepare catalysts with higher surface area and smaller particle size (Jung et al., 2004) .

The present work is designated to synthesize and characterize of cheaper, more abundant and highly active nanostructured metal oxide catalysts for the catalytic oxidation of CO to CO_2. The effects of catalyst composition, catalytic temperature, carbon monoxide concentration and weight of catalyst on the rate of catalytic CO oxidation reaction were also investigated and flowed up using advanced Quadruple gas mass analyzer system and the experimental data were used to clarify the mechanism of the catalytic oxidation reaction.

2. Experimental

2.1. Catalyst preparation Experiment

Different nanocrystallite materials of $CuO\text{-}CeO_2$ with molar ratio 5:95 and $CuO\text{-}Fe_2O_3$ with molar ratio1:1, were prepared by using co-precipitation method where the metal precursor's solutions (Cerium (III) sulphate, cupper (II) sulphate and iron (II) nitrate) with required molar ratio were co-precipitated using potassium hydroxide as a precipitating agent; the later was added drop wisely to the precursor's solutions during ultra sonication. After 30 minutes the obtained precipitate was washed with distilled water and ethanol, dried at 105^{o}C and finally fired at 500^{o}C for about 3 hrs.

Nanosized $CuO\text{-}CeO_2$ supported Al_2O_3 is prepared by weight impregnation technique (Avgouropoulos et al., 2002) where a catalyst of the composition 40% weight % of nano-sized $CuO\text{-}CeO_2$ was mixed with 60% weight % Al_2O_3 powder was prepared as follows: a suspension of nanosized $CuO\text{-}CeO_2$ was mixed with Al_2O_3 powder and stirred for 1 hr at 60 ^{o}C to form a paste and to achieve a homogeneous impregnation of catalyst in the Al_2O_3 support. The impregnate was then dried in an oven at 100 ^{o}C for 1 hr, calcinated at 400 ^{o}C for 3 hrs in a box muffle furnace.

Nanosized $CuO\text{-}Fe_2O_3\text{-}CeO_2\text{-}Al_2O_3$ with molar ratio 0.26: 0.19: 0.25: 0.3 was prepared by physical mixing of a solid mixture of one mole of $CuO\text{-}Fe_2O_3$ with one mole of $CuO\text{-}CeO_2\text{-}Al_2O_3$.

The prepared samples are characterized physically and chemically through X-ray diffraction, inductive coupled plasma-atomic emission spectroscopy (ICP-AES), BET surface area apparatus, transmission electron microscope (TEM) and scanning electron microscope (SEM).

Phase identification and crystallite size of the prepared catalysts were determined at room temperature by X-ray diffraction analysis was carried out for the prepared samples at room temperature and diffraction patterns were obtained by means of a chart recording Bruker ax5–D8 Advance–Diffrax plus search X-ray diffractometer using copper (Kα) radiation (λ=1.5406˚A) and secondary monochromator in the range 2θ from 10˚to 80˚. Crystallite size is automatically calculated from X-ray diffraction data using the diffraction peaks, computer software TOPAS 2 and the following Scherer's formula (Cullity and Stock, 2001):

$$D = \frac{0.9\lambda}{(\beta - \beta_1)\cos\theta}$$

Where D is the grain diameter, β the half-intensity width of the relevant diffraction peak, β_1 represents the half-intensity width due to instrumental broadening, λ the X-ray wave length, and θ_1 is the angle of diffraction

2.2. CO catalytic oxidation Experiment

The experimental apparatus for CO catalytic oxidation were constructed as follow a certain weight of the prepared catalysts is being inserted between two pieces of quartz wool in a tubular horizontal flow reactor (length 120 cm, i.d 1 cm). The reactor is heated in a tubular furnace up to the required catalytic temperature. The sample is kept at that temperature for about 20 min. before the onset of the experiment to refresh the catalyst. CO/O_2/Ar gas mixture was passed over the catalyst at a constant rate of 1l/min. Gas analyzer (QMS sample analysis HPR 20, Hidden-Analytical, Warrington, UK).was used for measuring gas concentration during CO catalytic oxidation reaction and the CO conversion % was estimated from the following equation:

$$\text{CO conversion \%} = \frac{CO_i - CO_t}{CO_i} x100$$

Where CO_i is the initial CO concentration and CO_t is the CO concentration at time t. The efficiency of the prepared powder as a catalyst for CO oxidation can be defined by the maximum degree of CO conversion %.

The efficiency of the prepared catalysts were determined and correlated with operation parameters which comprise; catalyst chemical composition, Temperature of reaction, CO initial concentrations and catalyst weights.

The effect of catalysts chemical composition and catalytic CO oxidation temperature were determined by carrying out the CO oxidation reactions over the previous prepared catalysts at temperature ranging from 300 - 500^{o}C.

The effect of CO initial concentrations on CO oxidation were determined by carrying out the catalytic reactions over CuO-CeO_2-Al_2O_3 using different CO inlet concentrations ranging from 5 to 16% catalyst at 500^{o}C.

The optimum weight of the most effective catalysts, which give the highest CO conversion %, was investigated using different catalyst weights ranging from 0.3 to 3 g at 300 ^{o}C. The effect of catalytic CO oxidation temperatures were carried out over the most effective catalyst and weight at temperature ranging from 100 - 500^{o}C.

The experimental data were used to clarify the mechanism of the catalytic oxidation reaction

.

3. Results and discussions

3.1. Characterizations of different catalysts

Phase identification and crystallite size of the products are shown in table 1 and fig.1.

Fig.1a shows XRD patterns of CuO-Fe_2O_3 catalysts, from which it is clear that there is no interaction between CuO and Fe_2O_3 and no copper ferrite peaks were detected.

Fig.1(b, c) show XRD patterns of CuO–CeO_2 catalysts washed with ethanol and CuO–CeO_2 supported alumina, the distinct fluorite-type oxide structure of CeO_2 was observed in all samples (Jung et al., 2004). In addition, no shift in the diffraction peaks of CeO_2 could be found in these catalysts, indicating that no solid solutions appeared in the CuO–CeO_2 catalyst. However, it should also be noted that the XRD peaks of CeO_2 were rather broad and shifts of small magnitude could be undetectable (Avgouropoulos et al., 2005), We found no observable XRD peaks corresponding cupper oxides. This could indicate that the doped CuO was uniformly dispersed in the CeO_2 matrix. Otherwise, they are amorphous or undetectable amount by XRD. The XRD results indicate also that the addition of KOH as precipitating agent inhibits the growth of CuO–CeO_2 particles, yields nano-structured catalysts (crystal size =12.7 nm) and increases the surface areas of catalysts (58.3 $m^2 g^{-1}$ for CuO–CeO_2)as summarized in table .1.

The results obtained from inductive coupled plasma-atomic emission spectroscopy indicate that the catalysts are well prepared with the proper metal-to-metal ratios as summarized in table.2.

Fig.2. and Fig.3. Shows TEM and SEM images of CuO-CeO_2 supported Al_2O_3 catalyst and CuO-Fe_2O_3 catalyst, from which we can see that the particles are well dispersed and have a regular spherical morphology, the powder was mostly formed in homogenous grains and CuO-Fe_2O_3 sample seems to be more condensed than CuO-CeO_2-Al_2O_3. The pore size distribution shown in Fig.4 and the data obtained from the BET surface area apparatus show that the total pore volume is 2.9 x10 $^{-2}$ CC / g, micro pore volume 6.6 x10 $^{-2}$ CC / g and average pore diameter 0.02 µm in case of CuO-CeO_2-Al_2O_3 while in case of CuO-Fe_2O_3 the total pore volume is 7.5 x10 $^{-3}$ CC / g , micro pore volume 1.3 x10 $^{-2}$ CC / g and average pore diameter 0.019 µm and this indicate that CuO-Fe_2O_3 sample is more dense than CuO-CeO_2-Al_2O_3

3.2. Catalytic oxidation test for removal of CO

3.2.1. Effect of catalyst chemical composition

Catalytic oxidation tests were carried out in the simulated reactor to study the effect of different operation parameters on the removal of CO using different nanosized materials. The oxidation tests were investigated isothermally through the oxidation of CO to CO_2 as a function of the prepared samples in the temperature range 300–500 ^{o}C.

It was observed from Table 3 and fig.5. that ceria containing catalysts give the highest efficiency at all the catalytic temperatures; this is due to its small crystal size and high surface area. Furthermore, ceria contains a high concentration of highly mobile oxygen vacancies, which act as local sources or sinks for oxygen involved in reactions taking place on its surface (Laosiripojana and Assabumrungrat, 2005).It was believed that the reaction is catalyzed by the interfacial copper oxide–ceria centers in which ceria presents a high number of oxygen vacancies

that permits a high mobility of lattice oxygen (Liu and Flytzanistephanopoulos, 1995; Wang et al., 2000).The high porosity value of ceria might be another factor for the high efficiency of the ceria containing catalysts.

3.2.2. Effect of catalytic temperature

The catalytic oxidation temperature is considered to be the main factor affecting the overall rate of conversion of CO to CO_2. The influence of catalytic oxidation temperatures on the rate of conversion of CO to CO_2 is shown in Fig.5. and table. 3. As time proceeds, CO conversion increases and the rate of conversion is high initially and slows down till the end of the reaction. At relatively lower temperature , 300 ^oC, the maximum CO oxidation occurs over $CuO\text{-}CeO_2\text{-}Al_2O_3$, $CuO\text{-}CeO_2$ and $CuO\text{-}CeO_2\text{-}Fe_2O_3\text{-}Al_2O_3$ catalysts and the conversion percent was about 72 , 60 and 48 % respectively, then it increases with increasing temperature to 400 ^oC and reaches about 100% over the three catalysts and this can be explained by the overheating of the active centers of the catalyst resulting from the liberation of excessive heat from the highly exothermic reaction of CO to CO_2 oxidation(Subbotin et al., 1999). At higher oxidation temperatures (450 and 500^oC), the CO conversion % decreases again and this phenomena can be attributed to the sintering effect whereas grain growth with partial coalescence takes place which decreases the number of active sites available for catalytic process (Abdel Halim et al., 2007).

Fig.6. summarizes the effect of temperature on the rate of catalytic CO to CO_2 conversion percent over all the prepared samples

To study the kinetics of catalytic oxidation reaction over the prepared metal oxides catalyst, the apparent activation energy for CO oxidation was calculated using Arrhenius equation(Li et al., 2003):

$$\ln[-\ln(1-x)] = \ln A + \ln\left[v/u\right] - \frac{E_a}{RT}$$

Where x is the carbon monoxide to carbon dioxide conversion rate, A is the pre-exponential factor in s^{-1}, u is the flow rate in ml s^{-1}, v is the total volume of the catalyst in cm^3, E_a is the apparent activation energy in kJ /mol, R is the gas constant and T is the absolute temperature in Kelvin. The value of activation energy can be calculated by plotting $\ln[-\ln(1-x)]$ versus 1/T for all samples as shown in Fig.7. It can be observed that the value of activation energy is relatively small in all samples containing ceria (3.7-7 kJ/mol), Such lower value of activation energy for catalysts containing ceria could be the reason for its high efficiency on CO oxidation, while $CuO\text{-}Fe_2O_3$ catalyst shows relatively high value of apparent activation energy (29.7 kJ/mol).

3.2.3. Effect of CO initial concentration

CO conversion % over $CuO\text{-}CeO_2\text{-}Al_2O_3$ increase with the decrease of CO concentration passing over the catalyst, where it increase from 84% to 100% by decreasing the carbon monoxide initial concentration from 16% to 5% over 0.3 g of $CuO\text{-}CeO_2\text{-}Al_2O_3$ catalyst at 500 ^oC and this is due to that with increasing the CO concentration the adsorbed CO molecules at the surface of the catalyst poison the active sites on the catalyst surface by covering and preventing it from direct contact with the flow gas.

3.2.4. CO oxidation mechanism

The XRD patterns for $CuO\text{-}CeO_2\text{-}Al_2O_3$ nanocatalyst after CO oxidation are shown in Fig.8. It can be reported that there is no difference between the phases formed before and after CO oxidation reaction and this indicates that the most possible mechanisms for CO oxidation on $CuO\text{-}CeO_2\text{-}Al_2O_3$ catalyst is the adsorption mechanism (Reddy et al., 2004a). Where in adsorption mechanism the reactants are adsorbed on the surface of the catalyst with breaking O-O bonds, then CO pick up the dissociated O atom forming CO_2 as represented by the following equations

$O_2 \leftrightarrow 2O$ (ads)

CO (gas) $\leftrightarrow$ CO (ads)

CO (ads) +O (ads) $\leftrightarrow$ CO_2 (ads)

CO_2 (ads) $\leftrightarrow$ CO_2 (gas)

3.2.5. Effect of catalyst mass

From the previous results obtained, it is clear that both $CuO\text{-}CeO_2\text{-}Al_2O_3$ and $CuO\text{-}CeO_2\text{-}Fe_2O_3\text{-}Al_2O_3$ are the most promising catalysts for the catalytic oxidation of CO to CO_2 and the effect of the catalyst mass on the CO conversion % at 300^oC was performed over them (Table 4). For $CuO\text{-}CeO_2\text{-}Al_2O_3$ and $CuO\text{-}CeO_2\text{-}Fe_2O_3\text{-}Al_2O_3$ catalysts, it was found that the CO conversion increased by increasing catalyst mass from, 0.3to 3 g and this may be attributed to the increase on the total surface area and the number of active sites on the catalyst surface which intern enhance the adsorption of CO and O_2 on the catalyst surface with breaking O-O bonds, then CO pick up the dissociated O atom forming CO_2.

The Effect of temperature on the CO conversion % over 3 g of $CuO\text{-}CeO_2\text{-}Al_2O_3$ and $CuO\text{-}CeO_2\text{-}Fe_2O_3\text{-}Al_2O_3$ catalysts using 5% CO initial concentration was studied and it was observed that the CO conversion % increases with increasing catalytic oxidation temperature as shown in table 5 and fig.9. where CO conversion % increases with increasing temperature as a result of overheating of the active centers of the catalyst and the lowering

in the activation energy with increasing weight and temperature where it decrease from 7 to 4.4 kJ/mol in case of $CuO-CeO_2-Al_2O_3$ and from 4.8 to 1.7 kJ/mol in case of $CuO-CeO_2-Fe_2O_3-Al_2O_3$ by changing the weight from 0.3 g to 3 g respectively (fig.10).

Table .1. Crystal sizes and surface area of the prepared catalysts

Catalyst	Sample phases	Crystal size (nm)	Surface area (m^2/g)
$CuO-Fe_2O_3$	CuO	28.7 nm	15.7
	Fe_2O_3	13.6 nm	
$CuO-CeO_2-Al_2O_3$	CuO	n.d	58.3
	CeO_2	11.7 nm	
	Al_2O_3	7 nm	
$CuO-CeO_2$	CuO	n.d	n.d
	CeO_2	12.7 nm	

n.d means Not determined

Table .2. ICP –AES results of the prepared catalysts

Catalyst	Chemical composition	ICP results ratios
1	50% CuO + 50% Fe_2O_3	51% CuO + 49% Fe_2O_3
2	5% CuO + 95% CeO_2	5.1% CuO + 94.9% CeO_2
3	2% CuO + 38% CeO_2+ 60% Al_2O_3	2% CuO + 39.1% CeO_2+ 58.9% Al_2O_3

Table .3. Effect of temperature on CO conversion % over 0.3 gram of catalyst (16 % CO initial flow rate)

Catalyst	300°C (CO Conv.%)	400°C (CO Conv.%)	450°C (CO Conv.%)	500°C (CO Conv.%)
$CuO-Fe_2O_3$	26	48	28.8	52.8
$CuO-CeO_2-Al_2O_3$	72	100	84	84
$CuO-CeO_2$	60	100	85	87
$CuO-CeO_2-Fe_2O_3-Al_2O_3$	48	96	98	99.7

Table .4 Effect of catalyst mass on the CO oxidation at 300 °C and 5% CO intial flow rate

Catalyst weight	0.3g	1g	2g	3g
CO conversion % over $CuO-CeO_2-Al_2O_3$	74 %	80 %	82 %	98 %
CO conversion % over $CuO-CeO_2-Fe_2O_3-Al_2O_3$	48 %	62 %	75 %	80 %

Table .5. Effect of temperature on CO conversion % over 3g of $CuO-CeO_2-Al_2O_3$ and $CuO-CeO_2-Fe_2O_3-Al_2O_3$ and CO gas flow rate of 50 ml/min (5%)

Temperature	100	200	300	400	500
CO conversion % over $CuO-CeO_2-Al_2O_3$	49.5%	82 %	95.3 %	99.9 %	100 %
CO conversion % over $CuO-CeO_2-Fe_2O_3-Al_2O_3$	57%	74 %	80 %	96 %	100 %

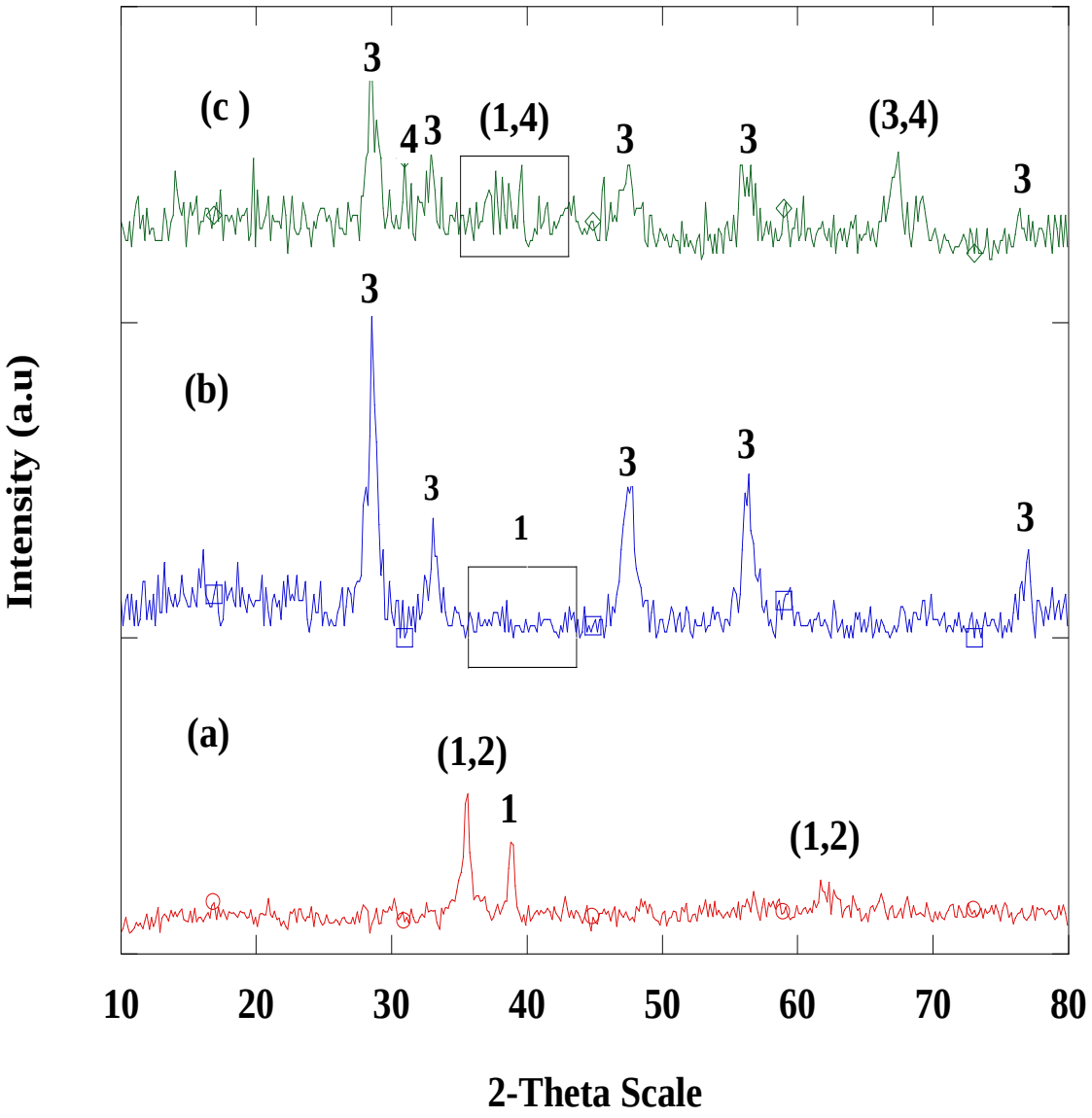

Fig .1. XRD pattern for
(a) CuO-Fe_2O_3 (b) CuO-CeO_2 (c) CuO-CeO_2-Al_2O_3
Where 1, 2, 3 and 4 represent CuO , Fe_2O_3, CeO_2 and Al_2O_3 respectively

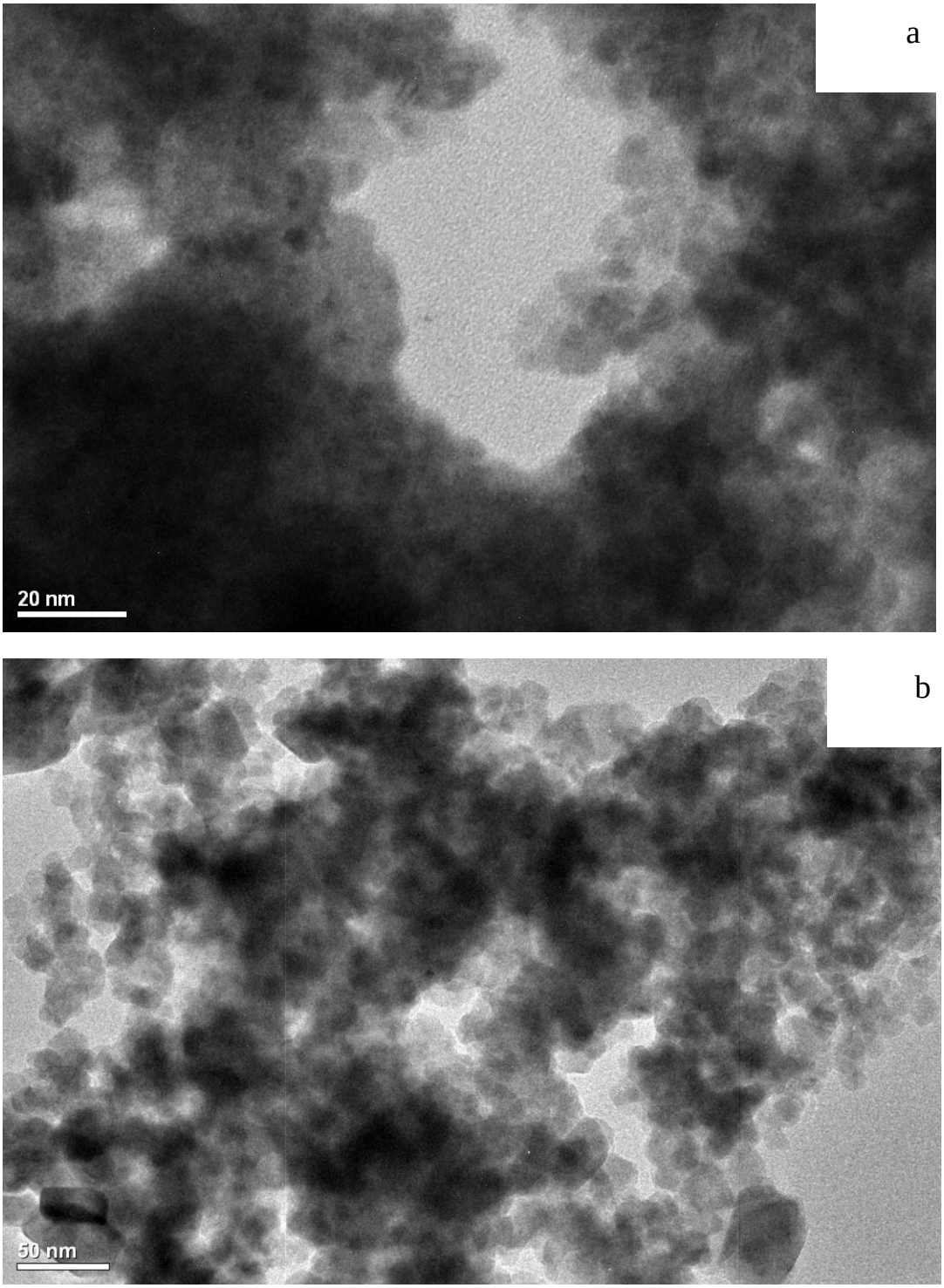

Fig .2. TEM image of
(a) CuO –CeO_2- Al_2O_3 (b) CuO –Fe_2O_3

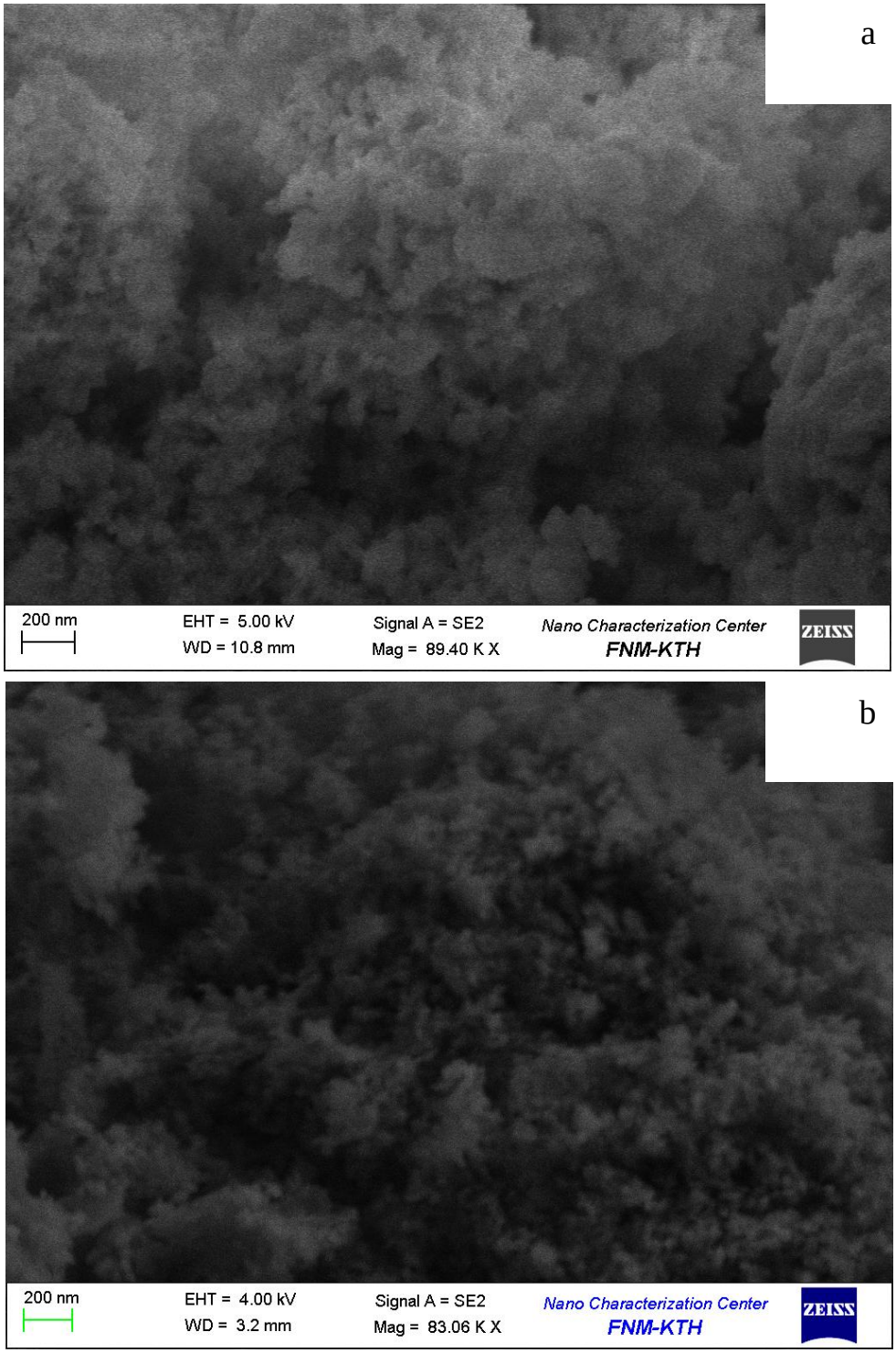

Fig .3. SEM image of
(a) CuO –CeO_2- Al_2O_3 (b) CuO –Fe_2O_3

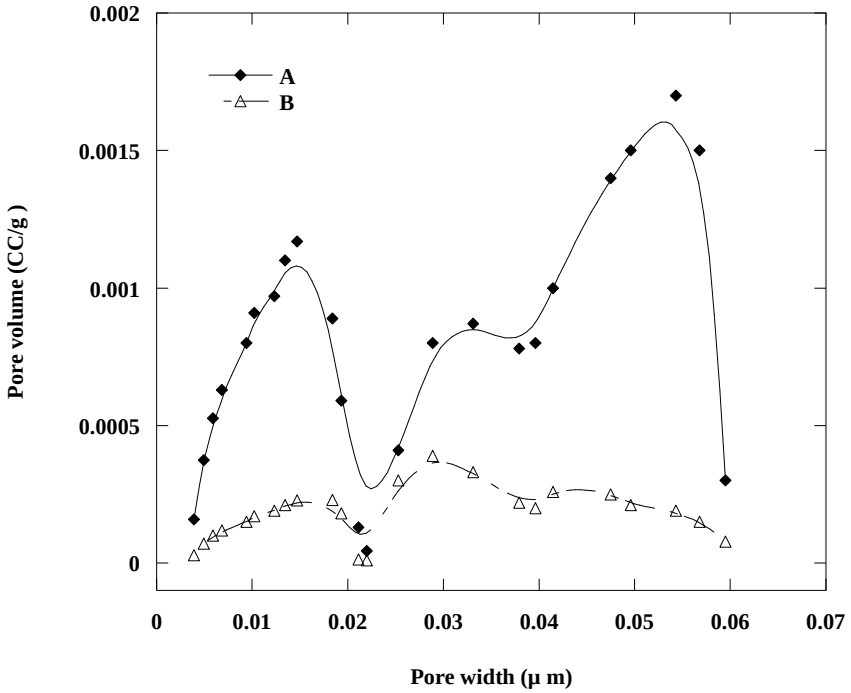

Fig. 4. Relation between pore volume and pore width for
(A) CuO -CeO_2-Al_2O_3 (B) CuO-Fe_2O_3

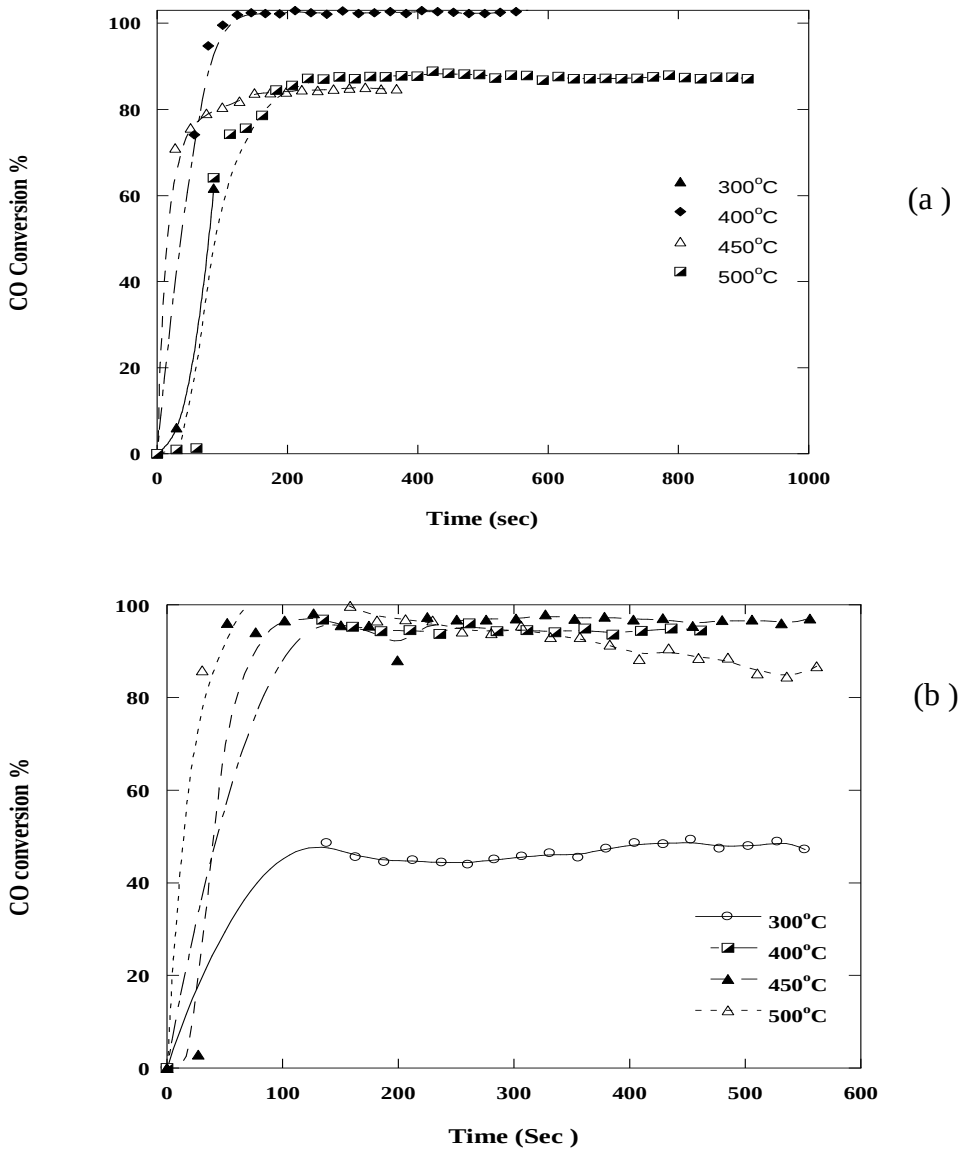

Fig.5. CO conversion % as a function of time at the temperature range 300–500 °C ;
(a)CeO_2-CuO (d) CuO -CeO_2-Fe_2O_3-Al_2O_3

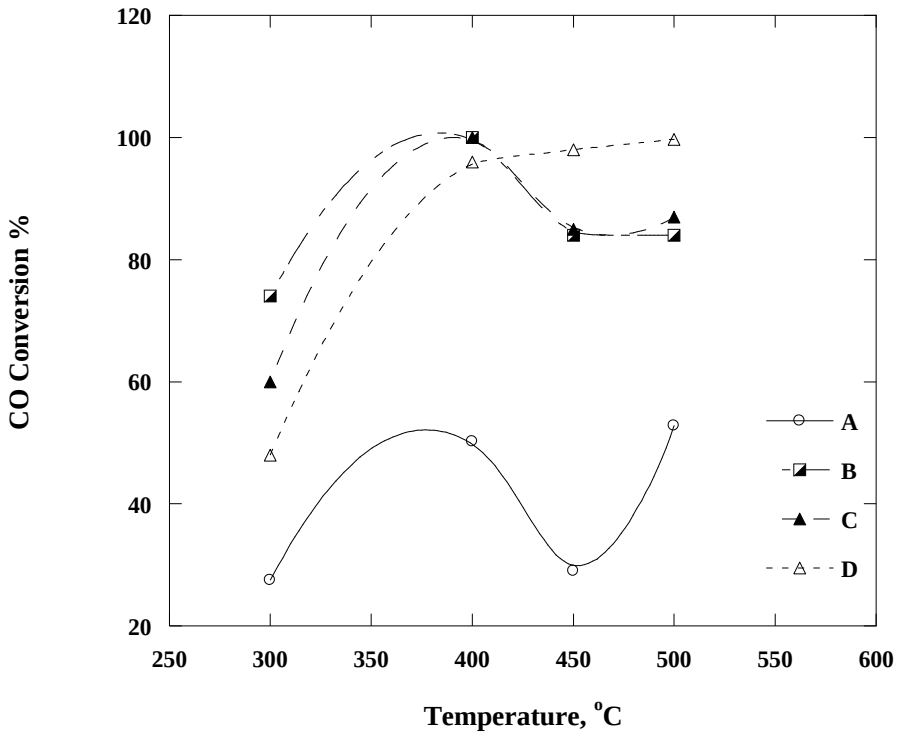

Fig.6. The relation between oxidation temperature and CO oxidation extent over:
(A) CuO -Fe_2O_3 (B) CuO -CeO_2-Al_2O_3
(C)) CuO -CeO_2 (D) CuO -CeO_2-Fe_2O_3-Al_2O_3

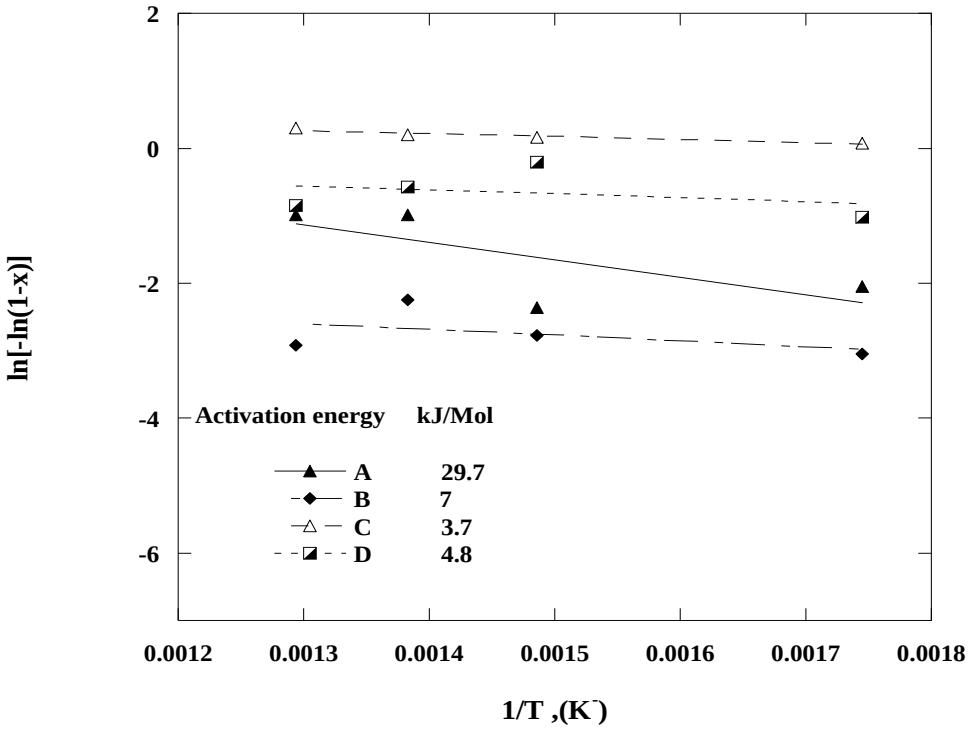

Fig. 7.Arrhenius plot for CO oxidation over
(A) CuO -Fe_2O_3 (B) CuO -CeO_2-Al_2O_3
(C) CuO -CeO_2 (D) CuO -CeO_2-Fe_2O_3-Al_2O_3

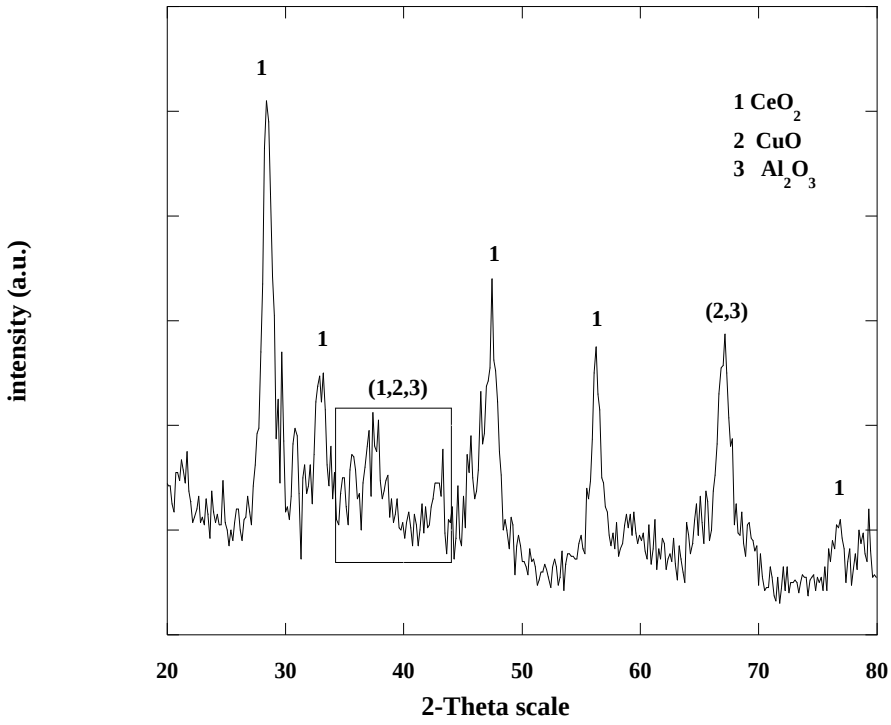

Fig.8 XRD patterns for CuO -CeO_2-Al_2O_3 after CO oxidation reaction

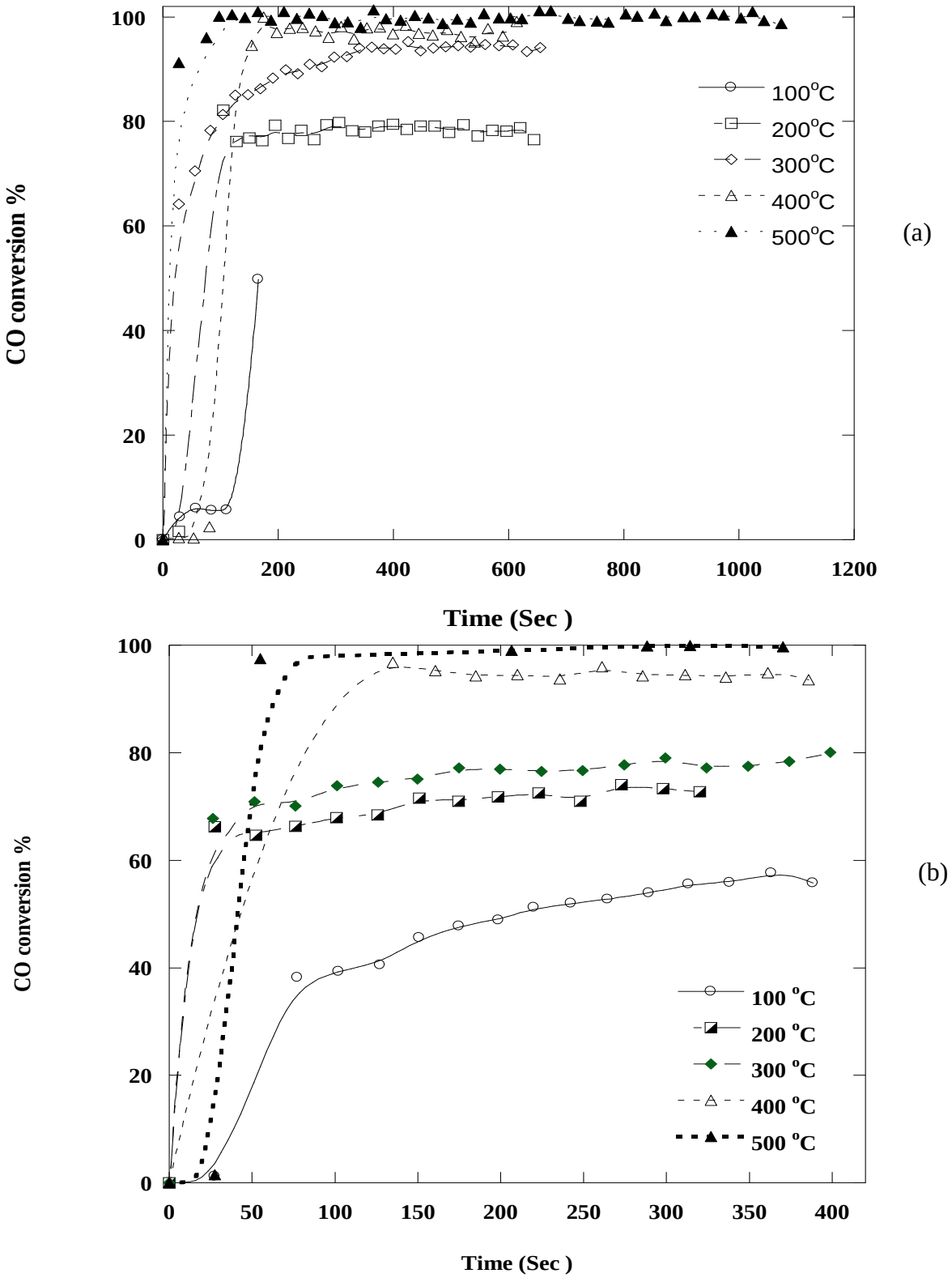

Fig .9. Effect of catalytic temperature on the CO oxidation at temperature range 300–500 °C and 5% CO intial flow rate over 3 g of

(a) CuO -CeO_2-Al_2O_3 (b) CuO -CeO_2-Fe_2O_3-Al_2O_3

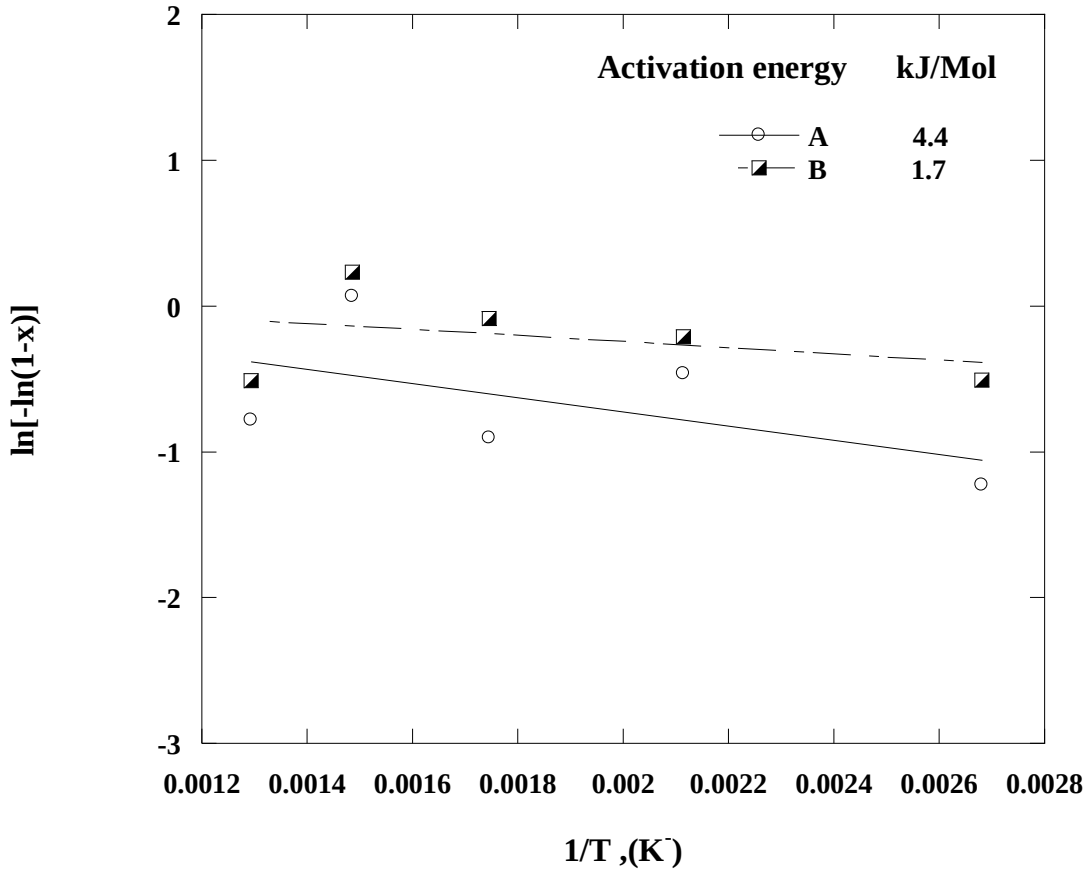

Fig.10.Arrhenius plot for CO oxidation over 3g and 5% CO initial flow rate at:
(A) CuO -CeO_2-Al_2O_3 (B) CuO -CeO_2-Fe_2O_3-Al_2O_3

Conclusion

CuO-CeO_2 and CuO-Fe_2O_3 were successfully prepared by co-precipitation route and CuO-CeO_2 was attached to the Al_2O_3 support to form CuO-CeO_2-Al_2O_3 using wet impregnation technique also CuO-Fe_2O_3-CeO_2-Al_2O_3 was prepared by physical mixing of one mole of CuO-CeO_2-Al_2O_3 with one mole of CuO-Fe_2O_3. , it was found that ceria containing catalysts give the highest efficiency in oxidation of CO to CO_2 at all the catalytic temperature. It was observed that the rate of CO oxidation to CO_2 increased by increasing catalytic temperature, at relatively lower temperature (300 ^oC), the maximum CO oxidation occurs over CuO-CeO_2-Al_2O_3, CuO-CeO_2 and CuO-CeO_2-Fe_2O_3-Al_2O_3 and with more increase of temperature to 450 and 500^oC the CO conversion % decrease again and this may be due to the sintering effect. it was also observed that CO conversion % over CuO-CeO_2-Al_2O_3 increase with the decrease of CO initial concentration and increasing catalyst weight. The study of the effect of temperature on CO conversion % over the most promising catalysts , CuO-CeO_2-Al_2O_3 and CuO-CeO_2-Fe_2O_3-Al_2O_3, using the optimum catalyst weight and the optimum CO initial concentration shows that the CO oxidation increase with increasing catalytic oxidation temperature . The experimental data shows that the catalytic oxidation of CO probably proceeded by adsorption mechanism where the reactants are adsorbed on the surface of the catalyst with breaking O–O bonds, then CO picks up the dissociated O atom forming CO_2

References

K. Abdel Halim, M. Khedr, M. Nasr and A. El-Mansy, Factors affecting CO oxidation over nanosized Fe_2O_3 , Materials research bulletin **42** (2007), pp. 731-741.

G. Avgouropoulos, T. Ioannides and H. Matralis, Influence of the preparation method on the performance of CuO-CeO_2 catalysts for the selective oxidation of CO, Applied Catalysis B: Environmental **56** (2005), pp. 87-93.

G. Avgouropoulos, T. Ioannides, H.K. Matralis, J. Batista and S. Hocevar, CuO-CeO_2 mixed oxide catalysts for the selective oxidation of carbon monoxide in excess hydrogen, Catalysis Letters **73** (2001), pp. 33-40.
G. Avgouropoulos, T. Ioannides, C. Papadopoulou, J. Batista, S. Hocevar and H. Matralis, A comparative study of Pt/g-Al_2O_3, Au/α-Fe_2O_3 and CuO-CeO_2 catalysts for the selective oxidation of carbon monoxide in excess hydrogen, Catalysis today **75** (2002), pp. 157-168.
T.V. Choudhary and D. Goodman, CO-free fuel processing for fuel cell applications, Catalysis today **77** (2002), pp. 65-78.
B.D .Cullity and S.R. Stock, Elements of X-ray Diffraction, Prentice hall Upper Saddle River, NJ (2001).
C. Dudfield, R. Chen and P. Adcock, A carbon monoxide PROX reactor for PEM fuel cell automotive application, International journal of hydrogen energy **26** (2001)pp. 763-775.
A. GLOBAL, Quantification of the disease burden attributable to environmental risk factors.
R. Gulyaev, E. Slavinskaya, S. Novopashin, D. Smovzh, A. Zaikovskii, D.Y. Osadchii, O. Bulavchenko, S. Korenev and A. Boronin, Highly active Pd CeO_x composite catalysts for low-temperature CO oxidation, prepared by plasma-arc synthesis, Applied Catalysis B: Environmental **147** (2014), pp. 132-143.
K.A. Halim, A. Ismail, M. Khedr and M. Abadir, Catalytic Oxidation of CO Gas over Nanocrystallite $Cu_x Mn_{1-x} Fe_2O_4$, Topics in Catalysis **47** (2008), pp. 66-72.
C.R. Jung, J. Han, S. Nam, T.-H. Lim, S.-A. Hong and H.-I. Lee, Selective oxidation of CO over CuO-CeO_2 catalyst: effect of calcination temperature, Catalysis today **93** (2004) pp. 183-190.
Y. Kang, X. Ye, J. Chen, L. Qi, R.E. Diaz, V. Doan-Nguyen, G. Xing, C.R. Kagan, J. Li and R.J. Gorte, Engineering Catalytic Contacts and Thermal Stability: Gold/Iron Oxide Binary Nanocrystal Superlattices for CO Oxidation, Journal of the American Chemical Society **135** (2013), pp. 1499-1505.
M.H. Khedr, K. Halim, M. Nasr and A. El-Mansy, Effect of temperature on the catalytic oxidation of CO over nano-sized iron oxide, Materials Science and Engineering: A **430** (2006), pp. 40-45.
D.H. Kim and J.E. Cha, A CuO-CeO_2 mixed-oxide catalyst for CO clean-up by selective oxidation in hydrogen-rich mixtures, Catalysis Letters **86** (2003), pp. 107-112.
N. Laosiripojana and S. Assabumrungrat, Catalytic dry reforming of methane over high surface area ceria ,Applied Catalysis B: Environmental **60** (2005), pp. 107-116.
P. Li, D.E. Miser, S. Rabiei, R.T. Yadav and M.R. Hajaligol, The removal of carbon monoxide by iron oxide nanoparticles, Applied Catalysis B: Environmental **43** (2003), pp. 151-162.
W. Liu and M .Flytzanistephanopoulos, Total Oxidation of Carbon Monoxide and Methane over Transition Metal Fluorite Oxide Composite Catalysts I. Catalyst Composition and Activity, Journal of Catalysis **153** (1995), pp. 304-316.
Y. Martynova, B.-H. Liu, M. McBriarty, I. Groot, M. Bedzyk, S. Shaikhutdinov and H.-J. Freund, CO oxidation over ZnO films on Pt (111) at near-atmospheric pressures, Journal of Catalysis **301** (2013), pp. 227-232.
C. Mathers, G. Stevens and M. Mascarenhas, Global health risks: mortality and burden of disease attributable to selected major risks, World Health Organization (2009).
W.H. Organization, Monitoring ambient air quality for health impact assessment, WHO Regional Publications, European Series (1999), p. 92.
N.C. Pérez, E.E. Miró and J.M. Zamaro, Cu, Ce/mordenite coatings on FeCrAl-alloy corrugated foils employed as catalytic microreactors for CO oxidation, Catalysis Today (2013).
M. Rashad, M. Khedr and K. Abdel-Halim, Magnetic and catalytic properties of Cu0. 5Zn0. 5Fe2O4 nanocrystallite powders, Journal of nanoscience and nanotechnology **6** (2006), pp. 114-119.
B. Reddy, F. Rasouli, M. Hajaligol and S. Khanna, Novel mechanism for oxidation of CO by Fe_2O_3 clusters, Fuel **83** (2004a), pp. 1537-1541.
B. Reddy, F. Rasouli ,M. Hajaligol and S. Khanna, Novel pathway for CO oxidation on a Fe_2O_3 cluster, Chemical physics letters **384** (2004b), pp. 242-245.
W. Shan, Z. Feng, Z. Li, J. Zhang, W. Shen and C. Li, Oxidative steam reforming of methanol on $Ce_{0.9} Cu_{0.1} O_Y$ catalysts prepared by deposition-precipitation, coprecipitation, and complexation-combustion methods, Journal of Catalysis **228** (2004), pp. 206-217.
A. Subbotin, B. Gudkov, Z.L. Dykh and V. Yakerson ,Temperature hysteresis in CO oxidation on catalysts of various nature, Reaction Kinetics and Catalysis Letters **66** (1999), pp. 97-104.
Y. Teng, H. Sakurai, A. Ueda and T. Kobayashi, Oxidative removal of CO contained in hydrogen by using metal oxide catalysts, International journal of hydrogen energy **24** (1999), pp. 355-358.
D.L. Trimm and Z.I. Ã–nsan, Onboard fuel conversion for hydrogen-fuel-cell-driven vehicles, Catalysis Reviews **43** (2001), pp. 31-84.

J.B. Wang, W.-H. Shih and T.-J. Huang, Study of Sm_2O_3 -doped CeO_2 /Al_2 O_3 -supported copper catalyst for CO oxidation, Applied Catalysis A: General **203** (2000), pp. 191-199.
G. Xia, Y. Yin, W. Willis, J. Wang and S. Suib, Efficient stable catalysts for low temperature carbon monoxide oxidation, Journal of Catalysis **185** (1999), pp. 91-105.